J|A|C|S ARTICLES

Published on Web 05/12/2010

Structures of $[Ag_7(SR)_4]^-$ and $[Ag_7(DMSA)_4]^-$

Hongjun Xiang,*,† Su-Huai Wei,‡ and Xingao Gong†

Key Laboratory of Computational Physical Sciences (Ministry of Education) and Department of Physics, Fudan University, Shanghai 200433, P. R. China, and National Renewable Energy Laboratory, Golden, Colorado 80401

Received December 23, 2009; E-mail: hxiang@fudan.edu.cn

Abstract: We have developed a new genetic algorithm approach to search for the global lowest-energy structures of ligand-protected metal clusters. In combination with density functional theory, our genetic algorithm simulations show that the ground state of $[Ag_7(DMSA)_4]^-$ has eight instead of four Ag−S bonds and has a much lower energy than the structure based on the $[Ag_7(SR)_4]^-$ cluster with a quasi-two-dimensional Ag_7 core. The simulated X-ray diffraction pattern of the $[Ag_7(DMSA)_4]^-$ cluster is in good agreement with the experimental result. Our calculations for the $[Ag_7(SR)_4]^-$ and $[Ag_7(DMSA)_4]^-$ clusters reveal for the first time that −RS−Ag−RS− can be a stable motif in thiolate-protected Ag clusters. In addition, the lowest-energy structures of $[Ag_7S_4]^-$, $[Ag_6S_4]^-$, and $[Ag_5S_4]^-$ are predicted.

Introduction

Metal nanoclusters might exhibit different optical and electronic properties from those of the bulk metals, making them appealing for applications in many fields, such as bioscience,[1,2] nanophotonics,[3] nanoelectronics,[4] and catalysis.[5,6] Ligand-protected metal nanoclusters, a new class of metallic materials at the nanometer scale, have received considerable attention because these clusters can be synthesized in macroscopic quantities and have pronounced stability in different environments and over a broad temperature range. Thiol-stabilized gold nanoclusters are being extensively studied because of their importance in both fundamental science[7−15] and technological applications.[16−18] For instance, the chirality of these materials has attracted much attention.[19] Some well-defined monodisperse thiolate-capped gold nanoclusters have been reported, and their structures have been determined by X-ray crystallographic analysis.[20−22] In particular, the Au core of the thiolate-protected $Au_{102}(p\text{-MBA})_{44}$ (p-MBA = $SC_7O_2H_5$) nanocluster was found to be packed in a Marks decahedron, surrounded by two types of "staple" motifs, namely, the simple motif −RS−Au−RS− and the extended motif −RS−Au−RS−Au−RS−.[20] A similar Au core/staple motif combination was also discovered in the $Au_{25}(SR)_{18}^-$ cluster, which possesses an icosahedral Au_{13} core and six −RS−Au−RS−Au−RS− extended staple motifs.[21−23]

Recently, silver nanoclusters have been found to exhibit interesting properties, such as strong fluorescence,[24−26] large solvatochromism,[27] broad multiband optical absorption,[28] and

† Fudan University.
‡ National Renewable Energy Laboratory.

(1) Gobin, A. M.; Lee, M. H.; Halas, N. J.; James, W. D.; Drezek, R. A.; West, J. L. *Nano Lett.* **2007**, *7*, 1929.
(2) Verma, A.; Uzun, O.; Hu, Y. H.; Hu, Y.; Han, H. S.; Watson, N.; Chen, S. L.; Irvine, D. J.; Stellacci, F. *Nat. Mater.* **2008**, *7*, 588.
(3) Haynes, C. L.; McFarland, A. D.; Zhao, L. L.; Van Duyne, R. P.; Schatz, G. C.; Gunnarsson, L.; Prikulis, J.; Kasemo, B.; Kall, M. *J. Phys. Chem. B* **2003**, *107*, 7337.
(4) Sivaramakrishnan, S.; Chia, P.-J.; Yeo, Y.-C.; Chua, L.-L.; Ho, P. K.-H. *Nat. Mater.* **2007**, *6*, 149.
(5) Daniel, M. C.; Astruc, D. *Chem. Rev.* **2004**, *104*, 293.
(6) Astruc, D.; Lu, F.; Aranzaes, J. R. *Angew. Chem., Int. Ed.* **2005**, *44*, 7852.
(7) Ingram, R. S.; Hostetler, M. J.; Murray, R. W. *J. Am. Chem. Soc.* **1997**, *119*, 9175.
(8) Chen, S. W.; Ingram, R. S.; Hostetler, M. J.; Pietron, J. J.; Murray, R. W.; Schaaff, T. G.; Khoury, J. T.; Alvarez, M. M.; Whetten, R. L. *Science* **1998**, *280*, 2098.
(9) Cleveland, C. L.; Landman, U.; Schaaff, T. G.; Shafigullin, M. N.; Stephens, P. W.; Whetten, R. L. *Phys. Rev. Lett.* **1997**, *79*, 1873.
(10) Wang, G.; Huang, T.; Murray, R. W.; Menard, L.; Nuzzo, R. G. *J. Am. Chem. Soc.* **2005**, *127*, 812.
(11) Negishi, Y.; Nobusada, K.; Tsukuda, T. *J. Am. Chem. Soc.* **2005**, *127*, 5261.
(12) Jin, R.; Egusa, S.; Scherer, N. F. *J. Am. Chem. Soc.* **2004**, *126*, 9900.
(13) Pei, Y.; Gao, Y.; Zeng, X. C. *J. Am. Chem. Soc.* **2008**, *130*, 7830.
(14) Pei, Y.; Gao, Y.; Shao, N.; Zeng, X. C. *J. Am. Chem. Soc.* **2009**, *131*, 13619.
(15) Jiang, D. E.; Tiago, M. L.; Luo, W. D.; Dai, S. *J. Am. Chem. Soc.* **2008**, *130*, 2777.
(16) Zheng, N.; Stucky, G. D. *J. Am. Chem. Soc.* **2006**, *128*, 14278.
(17) Fan, H.; Yang, K.; Boye, D. M.; Sigmon, T.; Malloy, K. J.; Xu, H.; Lopez, G. P.; Brinker, C. J. *Science* **2004**, *304*, 567.
(18) Rosi, N. L.; Giljohann, D. A.; Thaxton, C. S.; Lytton-Jean, A. K. R.; Han, M. S.; Mirkin, C. A. *Science* **2006**, *312*, 1027.
(19) (a) Noguez, C.; Garzón, I. L. *Chem. Soc. Rev.* **2009**, *38*, 757. (b) Gautier, C.; Bürgi, T. *ChemPhysChem* **2009**, *10*, 483. (c) Yao, H. *Curr. Nanosci.* **2008**, *4*, 92.
(20) Jadzinsky, P. D.; Calero, G.; Ackerson, C. J.; Bushnell, D. A.; Kornberg, R. D. *Science* **2007**, *318*, 430.
(21) Zhu, M.; Aikens, C. M.; Hollander, F. J.; Schatz, G. C.; Jin, R. *J. Am. Chem. Soc.* **2008**, *130*, 5883.
(22) Heaven, M. W.; Dass, A.; White, P. S.; Holt, K. M.; Murray, R. W. *J. Am. Chem. Soc.* **2008**, *130*, 3754.
(23) Akola, J.; Walter, M.; Whetten, R. L.; Häkkinen, H.; Grönbeck, H. *J. Am. Chem. Soc.* **2008**, *130*, 3756.
(24) Yu, J.; Choi, S.; Dickson, R. M. *Angew. Chem., Int. Ed.* **2009**, *48*, 318.
(25) Petty, J. T.; Zheng, J.; Hud, N. V.; Dickson, R. M. *J. Am. Chem. Soc.* **2004**, *126*, 5207.
(26) Richards, C. I.; Choi, S.; Hsiang, J. C.; Antoku, Y.; Vosch, T.; Bongiorno, A.; Tzeng, Y. L.; Dickson, R. M. *J. Am. Chem. Soc.* **2008**, *130*, 5038.
(27) Díez, I.; Pusa, M.; Kulmala, S.; Jiang, H.; Walther, A.; Goldmann, A. S.; Müller, A. H. E.; Ikkala, O.; Ras, R. H. A. *Angew. Chem., Int. Ed.* **2009**, *48*, 2122.

circular dichroism properties.[29] Unfortunately, the exact composition of these silver clusters could not be attained by mass spectrometry analysis. A breakthrough was achieved by Wu et al.,[30] who reported a high-yield synthesis of monodisperse thiolate-protected silver clusters and assigned the clusters as $[Ag_7(DMSA)_4]^-$, where DMSA represents *meso*-2,3-dimercaptosuccinic acid (see Figure 1a). However, the exact structure of $Ag_7(DMSA)_4$ has yet to be revealed because of the difficulty in growing single crystals of silver thiolate clusters. It is known that the DMSA group has two unsaturated S atoms (see Figure 1a). If only one of the two thiol groups in each DMSA ligand binds to the Ag_7 core, as suggested previously,[30] the $[Ag_7(DMSA)_4]^-$ cluster should have four delocalized valence electrons, in view of the fact that each thiolate ligand consumes one electron through Ag−S bond formation. According to the spherical jellium model,[31,32] bare alkaline or noble metal clusters with 2, 8, 20, etc., valence electrons should be highly stable because of closure of the electronic shell.[20−23] How a thiolate-protected Ag cluster can be stable without the closed-shell electronic structure remains a mystery. The other possibility is that both of the thiol groups in each of the DMSA ligands bind to the Ag_7 cluster. In this case, it would be unavoidable that some of the Ag atoms would have three or more neighboring S atoms. It is unclear whether the steric repulsion due to the large size of the DMSA group would lead to the instability of the whole cluster. In the following, we will refer to the above two different kinds of ligand-protected Ag clusters as $[Ag_7(SR)_4]^-$ and $[Ag_7(SRS)_4]^-$, respectively.

In this work, we have developed a new genetic algorithm (GA) to search for the lowest-energy structures of ligand-protected metal clusters. In combination with density functional theory (DFT), our approach was adopted to predict the structures of the $[Ag_7(SR)_4]^-$ and $[Ag_7(DMSA)_4]^-$ clusters. Our results show that the seven Ag atoms form a quasi-two-dimensional (quasi-2D) Ag-centered six-sided ring and that there are two simple −RS−Ag−RS− staple motifs in the $[Ag_7(SR)_4]^-$ cluster. Because the DMSA ligand has two unsaturated S atoms, $[Ag_7(DMSA)_4]^-$ takes a different but interesting structure: all of the thiol groups bind with the Ag_7 core, and the steric repulsion between the DMSA groups is very small. To the best of our knowledge, this represents the first theoretical attempt to predict the structures of thiolate-protected Ag clusters, and our theoretical investigations provide microscopic insight into the interactions between the thiol ligands and the Ag core.

Computational Method

GAs have been used to optimize geometries of nanoclusters since the 1990s.[33−36] They employ a search technique based on principles similar to those of natural selection, singling out the most "adaptive" clusters, which have the lowest energies.[34,37] Usually, all of the atoms in a cluster are treated on the same footing in a traditional GA simulation. In the case of ligand-protected metal clusters, it was found[20,21] that each ligand binds to the surface of the metal core cluster and that the relative arrangement of the atoms within a ligand remains almost unchanged. If we were to apply the usual GA approach to a metal cluster protected by a complex ligand such as *p*-MBA, finding the lowest-energy structure of the ligand-protected metal cluster would be computationally very demanding because of the large number of atoms. In order to search for the lowest-energy structure of the ligand-protected metal cluster in a more efficient way, we have proposed a new GA approach in which we treat the metal core and the ligands in different ways. For simplicity, we assume that only one atom of a ligand bonds with the metal core cluster (e.g., the sulfur atom binds with the Ag core in the case of the $-SCH_3$ group). It should be noted that our method can be also applied to the case of a ligand with several attaching atoms.

To clearly describe our new GA approach, we take the thiolate-protected $Ag_m(SCH_3)_n$ cluster as an illustrative example. To start a GA simulation, an initial population of structures is required. For each initial structure of the ligand-protected metal cluster, we first generate a randomly packed Ag_m cluster and then put n S atoms onto the surface of the Ag_m core in random positions. Finally, to each S atom we attach a CH_3 group. We use the Monte Carlo method to determine the orientation of the CH_3 group that minimizes the steric repulsion between the CH_3 group and other atoms. All of the clusters in the initial population are then relaxed into the nearest local minimum. To generate a new population, we perform the mating and mutation operations on parents chosen through the selection process.[37] For the mating and mutation operations, we consider only the Ag_mS_n part of the whole $Ag_m(SCH_3)_n$ cluster. After the operations, we add the CH_3 groups back into the newly generated Ag_mS_n cluster using the same Monte Carlo method mentioned above. For the mating operation, we closely follow the cut-and-splice method proprosed by Deaven and Ho.[34] In the mutation operation, we displace some atoms with a predefined probability. The next generation is chosen to be the p different lowest-energy clusters among the parents and offspring. The process is repeated until the ground-state structure is located. In this work, we set the population size to 16. Usually, 10 generations were sufficient to obtain the lowest-energy structures of the clusters considered in this work. We repeated the calculations several times to confirm each of the lowest-energy structures obtained.

In this study, we used DFT to calculate the energies and relax the structures. In our DFT plane-wave calculations, we used the generalized gradient approximation (GGA)[38] and a plane-wave cutoff energy of 400 eV. The ion−electron interaction was treated using the projector-augmented wave (PAW)[39] technique as implemented in the Vienna ab initio simulation package.[40] For relaxed structures, the atomic forces were less than 0.02 eV/Å. Cubic supercells with lattice constants large enough to avoid image interactions were adopted.

Results and Discussion

As discussed in the Introduction, there are two possible bonding mechanisms for the $[Ag_7(DMSA)_4]^-$ cluster. We will consider each of these scenarios in the following sections.

Ground-State Structure of $[Ag_7(SR)_4]^-$. First, we assumed that only half of the S atoms of the DMSA groups bond directly with the Ag core while the remaining S atoms form S−S bonds between neighboring DMSA groups. Therefore, to simplify the calculations, we first replaced the large DMSA group with the

(28) Bakr, O. M.; Amendola, V.; Aikens, C. M.; Wenselers, W.; Li, R.; Negro, L. D.; Schatz, G. C.; Stellacci, F. *Angew. Chem., Int. Ed.* **2009**, *48*, 5921.
(29) Nishida, N.; Yao, H.; Kimura, K. *Langmuir* **2008**, *24*, 2759.
(30) Wu, Z.; Lanni, E.; Chen, W.; Bier, M. E.; Ly, D.; Jin, R. *J. Am. Chem. Soc.* **2009**, *131*, 16672.
(31) Knight, W. D.; Clemenger, K.; de Heer, W. A.; Saunders, W. A.; Chou, M. Y.; Cohen, M. L. *Phys. Rev. Lett.* **1984**, *52*, 2141.
(32) de Heer, W. A. *Rev. Mod. Phys.* **1993**, *65*, 611.
(33) Hartke, B. *J. Phys. Chem.* **1993**, *97*, 9973.
(34) Deaven, D. M.; Ho, K. M. *Phys. Rev. Lett.* **1995**, *75*, 288.
(35) Ho, K.-M.; Shvartsburg, A. A.; Pan, B.; Lu, Z.-Y.; Wang, C.-Z.; Wacker, J. G.; Fye, J. L.; Jarrold, M. F. *Nature* **1998**, *392*, 582.
(36) Averkiev, B. B.; Zubarev, D. Y.; Wang, L. M.; Huang, W.; Wang, L. S.; Boldyrev, A. I. *J. Am. Chem. Soc.* **2008**, *130*, 9248.
(37) Johnston, R. L. *Dalton Trans.* **2003**, 4193.
(38) Perdew, J. P.; Burke, K.; Ernzerhof, M. *Phys. Rev. Lett.* **1996**, *77*, 3865.
(39) (a) Blöchl, P. E. *Phys. Rev. B* **1994**, *50*, 17953. (b) Kresse, G.; Joubert, D. *Phys. Rev. B* **1999**, *59*, 1758.
(40) Kresse, G.; Furthmüller, J. *Comput. Mater. Sci.* **1996**, *6*, 15. Kresse, G.; Furthmüller, J. *Phys. Rev. B* **1996**, *54*, 11169.

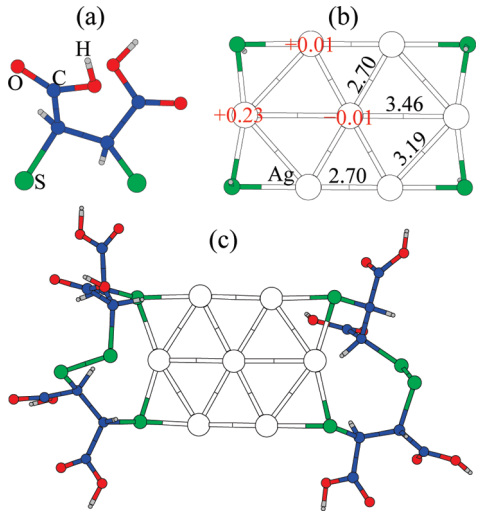

Figure 1. (a) Structure of the DMSA ligand. (b) Ground-state structure of the $[Ag_7(SR)_4]^-$ cluster from our GA simulations. The red numbers on the Ag atoms give the valence states determined using Bader charge analysis; the black numbers above the Ag−Ag bonds indicate the bond lengths in Å. (c) Lowest-energy structure **Is1** of the $[Ag_7(DMSA)_4]^-$ cluster constructed from the ground-state structure of the $[Ag_7(SR)_4]^-$ cluster.

SH group. The ground-state structure from our GA simulations is shown in Figure 1b. We can see that the seven Ag atoms form a quasi-2D cluster with apparent D_{6h} symmetry and that each S atom bonds with two neighboring peripheral Ag atoms. The $[Ag_7(SH)_4]^-$ structure can be also viewed as the addition of two −HS−Ag−HS− staples to the planar Ag_5 cluster. To the best of our knowledge, this is the first time that the −RS−Ag−RS− staple is revealed to be a stable motif in a thiolate-protected Ag cluster. The H atoms can be either below or above the Ag_7 plane because of the vanishingly small interaction between the SH groups. Therefore, there are several other clusters that are almost degenerate (within 20 meV) with the one shown in Figure 1b and have very similar electronic properties. Our additional GA simulations showed that the $[Ag_7(SCH_3)_4]^-$ cluster has a ground-state structure similar to that of the $[Ag_7(SH)_4]^-$ cluster, except for the replacement of H with CH_3.

To construct a model structure for the $[Ag_7(DMSA)_4]^-$ cluster based on the $[Ag_7(SH)_4]^-$ structure, we replaced each of the four SH groups with a DMSA ligand and tried to form S−S bonds between pairs of DMSA ligands. Several trial structures were constructed and relaxed. We found the structure shown in Figure 1c to have the lowest energy among the $[Ag_7(DMSA)_4]^-$ clusters with four Ag−S bonds. We hereafter refer to this structure as **Is1**. In this structure, two S atoms of the two DMSA ligands participate in the formation of an −RS−Ag−RS− staple, and the other two S atoms form a good S−S bond. Two connected DMSA groups lie above the Ag_7 cluster plane and the other two below the plane in order to minimize the steric repulsion. We note that the large size of the DMSA ligand should not change the basic framework of the Ag_7 cluster because the quasi-2D Ag_7 cluster is quite open. This is dramatically different from the case of Al clusters, where close-packed three-dimensional (3D) structures are preferred and the shape of the Al core can be controlled by the size of the ligand.[41]

(41) Xiang, H. J.; Kang, J.; Wei, S.-H.; Kim, Y.-H.; Curtis, C.; Blake, D. *J. Am. Chem. Soc.* **2009**, *131*, 8522.

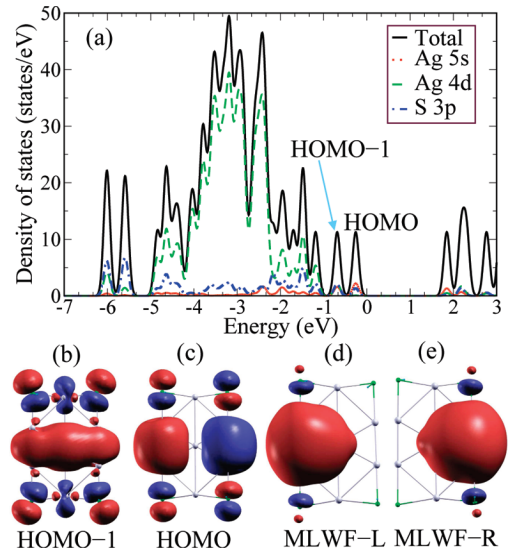

Figure 2. (a) Density of states (DOS) of the $[Ag_7(SH)_4]^-$ cluster. The partial DOSs are also shown. The DOS was calculated with 0.1 eV broadening. (b, c) Wave functions for the HOMO−1 and HOMO states. (d, e) Plots of the two maximally localized Wannier functions contributed mainly from the Ag 5s orbitals.

Electronic Structure of $[Ag_7(SR)_4]^-$. The electronic density of states (DOS) of the $[Ag_7(SH)_4]^-$ cluster is shown in Figure 2a. We can clearly see a large DFT band gap of ~2.1 eV, which is in accord with the ground-state nature of the structure. As expected, the occupied DOS is mostly contributed by Ag 4d orbitals, which are mainly distributed between −5 to −1 eV with respect to the highest occupied molecular orbital (HOMO) level. In addition, the two highest occupied molecular orbitals (HOMO−1 and HOMO) are well-separated from the region dominated by the Ag 4d states. Almost all of the occupied valence states have some contributions from the sulfur 3p states, indicating the hybridization between the S 3p and Ag 4d and 5s orbitals.

The wave functions of the HOMO−1 and HOMO states are shown in Figures 2b and c, respectively. For both the HOMO−1 and HOMO states, there are some small contributions from the S 2p orbitals, which interact in an antibonding fashion with the Ag atoms with one Ag−S bond. The HOMO−1 state is distributed mainly around the Ag atoms, with no more than one neighboring S atom, resulting in an elongated S-like orbital. Also, there is some small contribution from the 4d orbitals of the Ag atoms of the −RS−Ag−RS− staple, which is consistent with the partial DOS analysis. In contrast, the HOMO state is a P-like orbital with the nodal plane crossing the two Ag atoms of the two staples and oriented perpendicular to the Ag cluster plane, and there is almost no Ag 4d contribution. It is instructive to count the number of valence electrons in the cluster: each Ag atom contributes one 5s electron, and each thiolate consumes one electron through formation of the covalent Ag−S bond. In view of the charge state, the total number of valence electrons of the $[Ag_7(SH)_4]^-$ cluster is thus 4. It appears that the four valence electrons occupy the HOMO−1 S-like and HOMO P-like states.

To gain more insight into the electronic structure of the $[Ag_7(SH)_4]^-$ cluster, we calculated its maximally localized Wannier functions (MLWFs),[42] which were successfully used

(42) Marzari, N.; Vanderbilt, D. *Phys. Rev. B* **1997**, *56*, 12847.

to analyze the bonding.[43] The calculations were performed using the Quantum ESPRESSO[44] and Wannier90 codes.[45] Besides the Ag 4d-like and S sp^3 MLWFs, there are two unusual MLWFs, which are shown in Figure 2d,e. If the minor contribution from the S atom is disregarded, the two MLWFs are S-like orbitals whose centers are close to the centers of triangles made by three Ag atoms. The distribution of the two MLWFs is different from the usual MLWFs, which center on an atom or between two atoms. These two MLWFs look rather similar to each other, except that one (MWLF-L) is mainly distributed over the left side and the other (MWLF-R) over the right side. These two MLWFs yield two valence states: the bonding combination of MWLF-L and MWLF-R results in a low-lying state [i.e., the HOMO−1 state (Figure 2b)], whereas the antibonding interaction of MWLF-L with MWLF-R gives the HOMO state (Figure 2c) with a relatively higher energy.

According to the spherical jellium model, only clusters with a magic number of electrons are stable. As discussed above, the $[Ag_7(SR)_4]^-$ cluster has four valence electrons and thus should be unstable. However, our calculations also showed that the $[Ag_7(SR)_4]^-$ cluster has a DFT band gap larger than 1.8 eV, confirming its high stability. We attribute the large band gap and stability to the peculiar geometry of the cluster. In the $[Ag_7(SR)_4]^-$ cluster, the seven Ag atoms form a quasi-2D structure, which has a much lower symmetry than a 3D sphere. The addition of thiolate groups to the cluster results in a further lowering of the symmetry. As a matter of fact, the Ag atoms of the −RS−Ag−RS− staple have a different character from the other five Ag atoms: The distances between the atoms with two neighboring S atoms and other Ag atoms are larger than other Ag−Ag bond lengths (see Figure 1), and Bader charge analysis[46] showed that the Ag atoms with two neighboring S atoms lose significantly more electrons than the other Ag atoms (see Figure 1). Therefore, the $[Ag_7(SR)_4]^-$ cluster can be considered as the addition of two $[-RS-Ag-RS-]^-$ groups to the Ag_5^+ core. For the Ag_5^+ core, our GA simultions show that the lowest-energy form of the Ag_5^+ cluster (Figure 3a) can be looked upon as two Ag_2 units cross-linked by a central silver atom. We note that the Ag_5^+ cluster has HOMO−1 and HOMO states similar to those of the $[Ag_7(SR)_4]^-$ cluster. The only reasonable way to add an $[-HS-Ag-HS-]^-$ group is to connect the two S atoms to two Ag atoms that belong to different Ag triangles. Thus, we were able to form an initial structure for the $[Ag_7(SH)_4]^-$ cluster, as shown in Figure 3c. Relaxations of this structure would eventually lead to the ground-state structure of the $[Ag_7(SH)_4]^-$ cluster with the quasi-2D Ag_7 core (Figure 1b). This is due to the tendency to minimize the strain energy relative to the Ag−S bond lengths and Ag−S−Ag bond angles and the fact that the rotation of the Ag triangles around the central Ag atom in Ag_5^+ is essentially unhindered. Actually, the X-shaped planar D_{2h} Ag_5^+ cluster (Figure 3b) has only slightly higher energy (by ∼0.04 eV) than the D_{2d} structure (Figure 3a), in agreement with the previous calculations.[47]

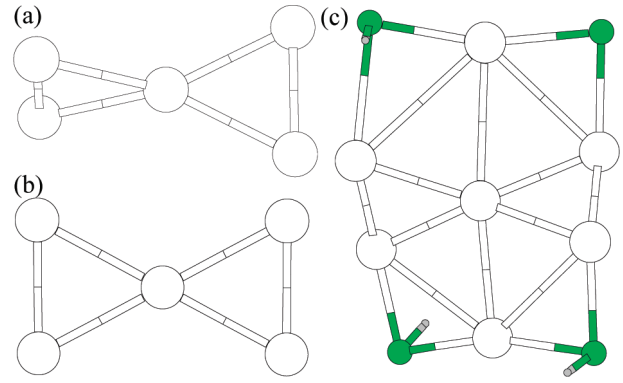

Figure 3. (a) Ground-state structure of the Ag_5^+ cluster with D_{2d} symmetry. (b) Low-energy structure of Ag_5^+ cluster with D_{2h} symmetry, whose energy is higher than that of the ground-state structure by only 40 meV. (c) Unrelaxed structure of the $[Ag_7(SH)_4]^-$ cluster constructed by adding two −HS−Ag−HS− staples to the ground-state structure of the Ag_5^+ cluster.

Our above discussion indicates that the electronic structure of the $[Ag_7(SR)_4]^-$ cluster is mainly determined by the D_{2h} X-shaped Ag_5^+ cluster. The lowering of the symmetry splits the threefold P states in the spherical Jellium model. As a matter of fact, in a pure 2D system, the P_z state does not exist. This explains the large band gap and stability of the cluster. Our argument is in the same spirit as the ellipsoidal shell model proposed by Clemenger,[48] although the ellipsoidal approximation is less applicable to clusters with less than 12 metal atoms.[48] Our results suggest that the "divide and protect" scheme[23,49] widely used to construct thiolate-protected Au clusters might be also applicable to thiolate-protected Ag clusters.

Ground-State Structure of $[Ag_7(SRS)_4]^-$. Here we consider the case where all of the thiol groups in the DMSA ligands bind to the Ag_7 cluster. The ground-state search was carried out using our new GA method for ligand-protected metal clusters. In order to correctly describe the steric effect caused by the large size of the DMSA group, we included the full structure of the DMSA ligands in the calculations. In the structural optimizations, all of the atoms, including the DMSA ligands, were fully relaxed. It should be noted that the DMSA ligands maintained the basic structure with no bond breaking after the optimizations. Through extensive GA simulations, the interesting structure shown in Figure 4 was revealed to be the lowest-energy structure for the $[Ag_7(SRS)_4]^-$ case. In this structure (designated as **Is2**), there are two DMSA−Ag_2−DMSA blocks. In a DMSA−Ag_2−DMSA block, the two S atoms of each DMSA group bond with the Ag_2 dimer. One DMSA−Ag_2−DMSA block can also be considered as two connected −RS−Ag−RS− staples. The whole structure of $[Ag_7(DMSA)_4]^-$ can also be viewed as the insertion of a Ag_3 trimer between two DMSA−Ag_2−DMSA blocks. The seven Ag atoms form a corner-shared double tetrahedron. In each of the tetrahedrons, the bond length of 3.39 Å between the two Ag atoms in the DMSA−Ag_2−DMSA block is larger than the others (∼3.0 Å). It is interesting that the $[Ag_7(DMSA)_4]^-$ structure is chiral because of the lack of improper rotations.

It can be seen that the $[Ag_7(DMSA)_4]^-$ structure has some favorable features: (1) each S atom bonds with two Ag atoms, since there are two Ag atoms that have three neighboring S

(43) Boero, M.; Terakura, K.; Ikeshoji, T.; Liew, C. C.; Parrinello, M. *Phys. Rev. Lett.* **2000**, *85*, 3245.
(44) Giannozzi, P.; et al. *J. Phys.: Condens. Matter* **2009**, *21*, 395502; http://www.quantum-espresso.org.
(45) Mostofi, A. A.; Yates, J. R.; Lee, Y.-S.; Souza, I.; Vanderbilt, D.; Marzari, N. *Comput. Phys. Commun.* **2008**, *178*, 685.
(46) Bader, R. F. W. *Atoms in Molecules: A Quantum Theory*; Oxford University Press: Oxford, U.K., 1990.
(47) Weis, P.; Bierweiler, T.; Gilb, S.; Kappes, M. M. *Chem. Phys. Lett.* **2002**, *355*, 355.
(48) Clemenger, K. *Phys. Rev. B* **1985**, *32*, 1359.
(49) Häkkinen, H.; Walter, M.; Grönbeck, H. *J. Phys. Chem. B* **2006**, *110*, 9927.

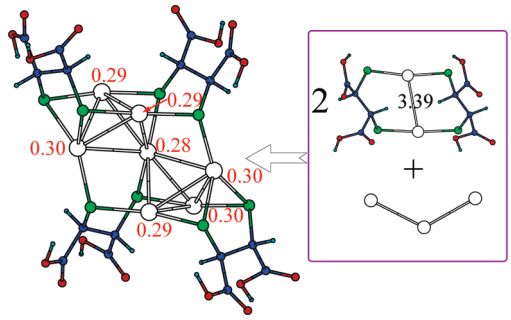

Figure 4. Ground-state structure (**Is2**) of the $[Ag_7(DMSA)_4]^-$ cluster with eight Ag−S bonds from the GA simulations. The red numbers near the Ag atoms give the valence states of the Ag atoms determined using Bader charge analysis. The right panel shows that the $[Ag_7(DMSA)_4]^-$ structure can be viewed as the addition of a Ag_3 trimer between two DMSA−Ag_2−DMSA blocks. The distance of 3.39 Å between the two Ag atoms in the DMSA−Ag_2−DMSA block is also shown.

atoms; (2) the steric repulsion in the cluster is vanishingly small because of the large separation between DMSA groups; (3) the number of Ag−Ag bonds (12) is the same as that in $[Ag_7(SH)_4]^-$; and (4) all of the Ag atoms are well-protected by the DMSA ligands, in contrast to the case of the quasi-2D Ag_7 core. An important finding from the simulation is that the lowest-energy $[Ag_7(DMSA)_4]^-$ structure with eight Ag−S bonds (Figure 4) has a much lower energy (by ∼3.57 eV) than the one with four Ag−S bonds (Figure 1c). Therefore, our results suggest that in the $[Ag_7(DMSA)_4]^-$ cluster, it is most probable that all of the thiol groups in the DMSA ligands bind to the Ag_7 cluster.

To qualitatively understand why the $[Ag_7(DMSA)_4]^-$ cluster with eight Ag−S bonds is so much more stable than that with four Ag−S bonds, we calculated the bond energies (E_b) of the Ag−S and S−S bonds. The bond energies were estimated in the following way:

$$E_b(\text{Ag−S}) = E(\text{Ag}) + E(\text{DMSA−H}) - E(\text{Ag−DMSA−H})$$
$$E_b(\text{S−S}) = 2E(\text{DMSA−H}) - E(\text{H−DMSA−DMSA−H}) \quad (1)$$

where E represents the total energy and DMSA−H denotes a DMSA ligand with one S atom passivated by one H atom. Our calculations show that the Ag−S and S−S bond energies are comparable: E_b(Ag−S) = 2.50 eV and E_b(S−S) = 2.74 eV. In view of the fact that the $[Ag_7(DMSA)_4]^-$ cluster with four Ag−S bonds has only two S−S bonds, it is clear that the $[Ag_7(DMSA)_4]^-$ cluster with eight Ag−S bonds is more stable.

Electronic Structure of $[Ag_7(DMSA)_4]^-$. The total and partial DOSs of $[Ag_7(DMSA)_4]^-$ are shown in Figure 5a. Comparison with the $[Ag_7(SH)_4]^-$ case shows that there is strong hybridization between the S 3p and Ag 5d orbitals with a negligible Ag 5s contribution to the occupied states. The smaller Ag 5s contribution is in accord with the fact that the $[Ag_7(DMSA)_4]^-$ cluster with eight Ag−S bonds has a lower energy, since it is well-known that the Ag 5s orbital has a higher energy than the S 3p orbitals. The HOMO states are twofold-degenerate, whereas the LUMO state is nondegenerate. The HOMO−LUMO gap is as large as 2.3 eV. The wave function plots show that the HOMO states are antibonding combinations of the S 3p orbitals and 4d orbitals of the Ag atom with three neighboring S atoms, whereas the LUMO state mainly consists of the corner Ag 5s orbital with some S 3p character. Bader analysis showed that the charge state of the Ag atoms is about +0.3, which is

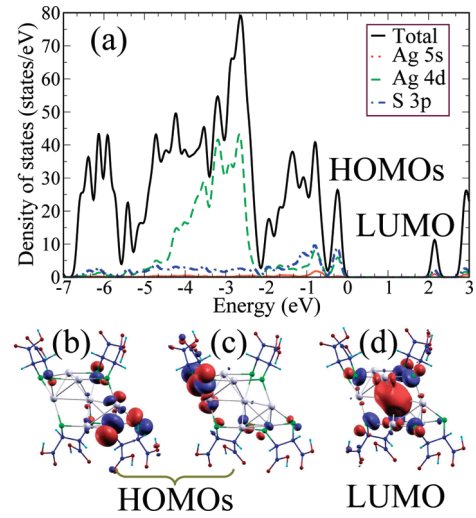

Figure 5. (a) DOS and partial DOS plots for the $[Ag_7(DMSA)_4]^-$ cluster. The DOSs were calculated with 0.1 eV broadening. (b, c) Wave functions for the twofold-degenerate HOMO states. (d) Wave function for the LUMO state.

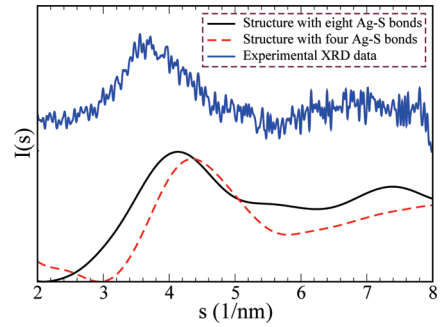

Figure 6. Simulated XRD patterns of **Is1** and **Is2** and the measured XRD pattern.[50]

much smaller than the nominal valence state of +1. This evidences the strong covalency of the Ag−S bond.

X-ray Diffraction Patterns. The X-ray diffraction (XRD) patterns of **Is1** and **Is2** were computed and compared with the experimental result.[50] The simulated XRD patterns were calculated using Debye function analysis.[14] The same parameters adopted by Pei et al.[14] were used, except that the wavelength λ was set to the experimental value of 0.15418 nm.[50] Our simulated XRD patterns are shown in Figure 6. It can be seen that major diffraction peaks in the experimental XRD pattern are well-reproduced by the XRD pattern of **Is2**. However, there are significant differences between the experimental result and the XRD pattern of **Is1**; in particular, the XRD pattern of **Is1** has a big dip at ∼3 nm^{-1} that is totally absent in the experimental pattern. Therefore, the simulation of the XRD patterns further confirms that the $[Ag_7(DMSA)_4]^-$ cluster probably has the **Is2** structure.

Ground-State Structures of $[Ag_7S_4]^-$, $[Ag_6S_4]^-$, and $[Ag_5S_4]^-$. Experimentally, smaller fragments such as $[Ag_7S_4]^-$, $[Ag_6S_4]^-$, and $[Ag_5S_4]^-$ were observed when the $[Ag_7(DMSA)_4]^-$ ion was subjected to collision at different energies. Here we discuss the ground-state structures of the $[Ag_mS_4]^-$ clusters with m = 5, 6, and 7. GA simulations were performed to search for the lowest-energy configurations of the $[Ag_mS_4]^-$

(50) Jin, R. Private communication.

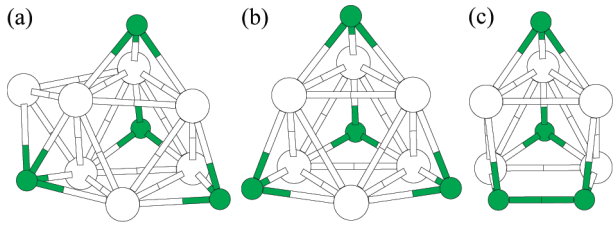

Figure 7. Ground-state structures of (a) $[Ag_7S_4]^-$, (b) $[Ag_6S_4]^-$, and (c) $[Ag_5S_4]^-$ from the GA simulations.

clusters. $[Ag_6S_4]^-$ was found to have a tetrahedral ground-state structure, as shown in Figure 7b. In the tetrahedron, the four S atoms are located at the corners, and each of the six Ag atoms sits in the middle of one edge. Therefore, each S atom has three neighboring Ag atoms. This structure can also be described as the addition of four S atoms to the octahedral Ag_6 cluster. Our calculations showed that the ground-state structures of both $[Ag_7S_4]^-$ and $[Ag_5S_4]^-$ can be constructed from the $[Ag_6S_4]^-$ cluster. Adding one Ag atom to one of the surfaces of the tetrahedral $[Ag_6S_4]^-$ cluster affords the ground-state structure of $[Ag_7S_4]^-$ (Figure 7a). In the ground-state structure, one S atom moves toward the additional Ag atom to form a new Ag−S bond. Removing one Ag atom from the $[Ag_6S_4]^-$ cluster gives the ground-state structure of $[Ag_5S_4]^-$ with a S−S bond (Figure 7c). The structural similarity among the $[Ag_mS_4]^-$ clusters naturally explains the experimental observation of the fragments.[30]

It is interesting to note that the $[Ag_7S_4]^-$ cluster takes a close-packed structure as the ground state, in sharp contrast to the rather open structure of the Ag_7S_4 part of the $[Ag_7(DMSA)_4]^-$ cluster with corner-shared double tetrahedrons. This occurs because the S atom of the DMSA (or SR) group prefers to bind with two Ag atoms, whereas the isolated S atom tends to form as many bonds as possible with Ag atoms in order to gain more electrons.

Conclusion

In conclusion, a novel, general genetic algorithm approach to search for the global lowest-energy structures of ligand-protected metal clusters has been developed. Our genetic algorithm simulations combined with DFT calculations have shown that the ground-state structure of the $[Ag_7(SR)_4]^-$ cluster can be viewed as the addition of two −RS−Ag−RS− staples to a D_{2h} planar Ag_5 cluster. The ground state of $[Ag_7(DMSA)_4]^-$ with eight Ag−S bonds has a much lower energy than the structure based on the $[Ag_7(SR)_4]^-$ cluster. In both the $[Ag_7(SR)_4]^-$ and $[Ag_7(DMSA)_4]^-$ clusters, there are −RS−Ag−RS− staples; in the $[Ag_7(DMSA)_4]^-$ cluster, each pair of staples forms a DMSA−Ag_2−DMSA block. The simulated X-ray diffraction pattern of the $[Ag_7(DMSA)_4]^-$ cluster is in good agreement with the experimental result. Furthermore, the ground-state structures of $[Ag_mS_4]^-$ clusters with $m = 5$, 6, and 7 have been predicted. Our study paves the way for reliable prediction of the structures and properties of ligand-protected metal clusters.

Acknowledgment. We thank Professor Rongchao Jin for helpful discussions and sending the unpublished experimental XRD pattern for the $[Ag_7(DMSA)_4]^-$ cluster. This work was partially supported by the National Science Foundation of China, the Program for Professor of Special Appointment (Eastern Scholar) at Shanghai Institutions of Higher Learning, the special funds for major state basic research, and the Shanghai municipality and MOE. Work at NREL was supported by the U.S. Department of Energy under Contract DE-AC36-08GO28308.

Supporting Information Available: Complete ref 44. This material is available free of charge via the Internet at http://pubs.acs.org.

JA9108374